

Parameters and Winds of Hot Massive Stars

By **ROLF P. KUDRITZKI**
AND **MIGUEL A. URBANEJA**

Institute for Astronomy, University of Hawaii, 2680 Woodlawn Drive, Honolulu, HI 96822, USA

Over the last years a new generation of model atmosphere codes, which include the effects of metal line-blanketing of millions of spectral lines in NLTE, has been used to re-determine the properties of massive stars through quantitative spectral analysis methods applied to optical, IR and UV spectra. This has resulted in a significant change of the effective temperature scale of early type stars and a revision of mass-loss rates. Observed mass-loss rates and effective temperatures depend strongly on metallicity, both in agreement with theoretical predictions. The new model atmospheres in conjunction with the new generation of 10m-class telescopes equipped with efficient multi-object spectrographs have made it possible to study blue supergiants in galaxies far beyond the Local Group in spectroscopic detail to determine accurate chemical composition, extinction and distances. A new distance determination method, the flux weighted gravity - luminosity relationship, is discussed as a very promising complement to existing stellar distance indicators.

Observationally, there are still fundamental uncertainties in the determination of stellar mass-loss rates, which are caused by the fact that there is evidence that the winds are inhomogeneous and clumped. This may lead to major revisions of the observed rates of mass-loss.

1. Introduction

Hot massive stars are cosmic engines of fundamental importance not only in the local but also in the early universe. A first generation of very massive stars has very likely influenced the formation and evolution of the first building blocks of galaxies. The spectral appearance of Lyman break galaxies and Ly α -emitters at high redshift is dominated by an intrinsic population of hot massive stars. Gamma-ray bursters are very likely the result of terminal collapses of very massive stars and may allow to trace the star formation history of the universe to extreme redshifts.

It is obvious that the understanding of important processes of star and galaxy formation in the early universe is intimately linked to our understanding of the physics of massive stars. The observational constraints of the latter are provided by quantitative spectroscopic diagnostics of the population of hot massive stars in the local universe. It is the goal of this contribution to provide an overview about the dramatic progress, which has been made in this field over the last five years.

There are two factors which have contributed to this progress, new observational facilities such as the optical/infrared telescopes of the 10m-class on the ground and observatories in space allowing for spectroscopy in the UV (HST, FUSE, GALLEX), IR (ISO, Spitzer) and at X-ray wavelengths (XMM, Chandra) and the enormous advancement of model atmosphere and radiative transfer techniques. As for the latter, it is important to realize that modelling the atmospheres of hot stars is a tremendous challenge. Their physics are complex and very different from standard stellar atmosphere models. They are dominated by a radiation field with energy densities larger than or of the same order as the energy density of the atmospheric matter. This has two important consequences. First, severe departures from Local Thermodynamic Equilibrium of the level populations in the entire atmosphere are induced, because radiative transitions between ionic energy levels become much more important than inelastic collisions. Second, supersonic hydrodynamic outflow of atmospheric matter is initiated by line absorption of photons

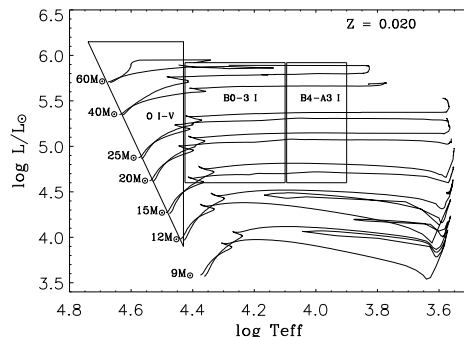


FIGURE 1. Evolutionary tracks of massive stars in the HRD with (solid) and without (dashed) stellar rotation, Meynet & Maeder (2000) and the domains of spectral types discussed in this review.

transferring outwardly directed momentum to the atmospheric plasma. This latter effect is responsible for the existence of the strong stellar winds observed and requires the use of NLTE model atmospheres, which include the hydrodynamic effects of stellar winds (see Kudritzki (1998) for a detailed description of the physics of hot star atmospheres).

The winds of hot massive stars are fundamentally important. Their energy and momentum input into the ISM is significant creating circumstellar shells, stellar wind bubbles and initiating further star formation. They affect the stellar evolution by modifying evolutionary timescales, chemical profiles, surface abundances and stellar luminosities. They also have substantial effects on the structure of the stellar atmospheres. They dominate the density stratification and the radiative transfer through their transonic velocity fields and they modify the amount of the emergent ionizing radiation significantly (Gabler et al., 1989, 1991, 1992, Najarro et al., 1996).

While the basic concepts for the hydrodynamic atmospheres of hot stars and the spectroscopic diagnostics of their parameters and stellar winds have been developed in the eighties and nineties (see reviews by Kudritzki & Hummer (1990), Kudritzki (1998) and Kudritzki & Puls (2000)), the development of the most recent generation of model atmospheres, which for the first time accounts selfconsistently for the effects of NLTE metal line-blanketing (see section 2), has lead to a dramatic change of the diagnostic results. A new effective temperature scale has been obtained for the O-star spectral types, which are apparently significantly cooler than originally assumed and, thus, on average have a lower luminosity and mass and also provide less ionizing photons, than previously thought. We will discuss these effects in detail in section 2, 3, and 4. Note that we will focus our review on “normal” hot massive stars in a mass-range between 15 and 100 M_{\odot} in well-established evolutionary stages such as dwarfs, giants, and supergiants (Fig. 1). We will not discuss objects with extreme winds such as Wolf-Rayet stars, luminous blue variables in outbursts, etc. For those, we refer the reader to the contributions by Paul Crowther and Nathan Smith in this volume.

The new model atmospheres in conjunction with the new generation of 10m-class telescopes equipped with efficient multi-object spectrographs allow to study blue supergiants in galaxies far beyond the Local Group in great spectroscopic detail to determine accurate chemical composition, extinction and distances. We will report recent results in this new field of “extragalactic stellar astronomy” in section 5. In section 6, we will discuss a new distance determination method based on stellar photospheric spectroscopy, the flux weighted gravity - luminosity relationship.

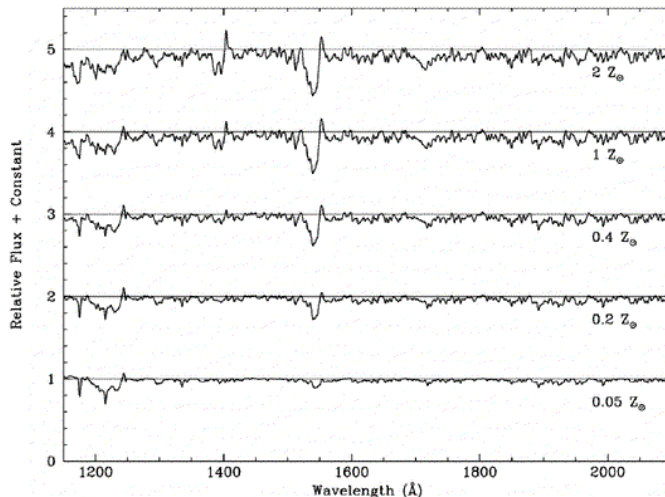


FIGURE 2. Model UV spectra of an integrated population of massive stars in a starburst galaxy displayed as a function of metallicity. The model atmosphere code used was WMBasic (Pauldrach, Lennon & Hoffmann (2001)) and the population synthesis was done with Starburst99. (From Rix, Pettini, Leitherer et al. (2004)).

The diagnostics of stellar winds, in particular of mass-loss rates, are also affected by the proper accounting for line-blanketing affects. While the general scaling relations of stellar wind parameters with stellar luminosity, mass, radius, and metallicity as described in Kudritzki & Puls (2000) remain qualitatively unchanged, important quantitative changes have been found. There are still puzzling uncertainties with regard to the observed rates of mass-loss related to the inhomogeneous structure of the stellar wind outflows. We will present and discuss the most recent results in section 7.

As indicated above, the new generation of model atmosphere codes has important applications on the interpretation of spectra of star-bursting galaxies in the early universe. Fig. 2 is a nice example. This work by Rix, Pettini, Leitherer et al. (2004) has been used to constrain star formation rates and metallicities in high redshift Lyman-break galaxies. Another example is the work by Barton et al. (2004), which uses stellar atmosphere model predictions by Bromm, Kudritzki & Loeb (2001) and Schaerer (2003) to explore the possibility to detect the first generation of very massive stars at redshifts around ten with present day 8m-class telescopes and with future (diffraction limited) optical/IR telescopes of 30m aperture such as the GSMT (see also report by the GSMT Science Working Group, Kudritzki et al. (2003a)). As it turns out, not only would the GSMT be able to detect such objects it would also allow to constrain the IMF of massive stars in the early universe from the relative comparison of L_α and HeII1640 recombination lines caused by the population of the first stars.

2. The effects of metal line blanketing

The inclusion of the opacity of millions of spectral lines in NLTE has two major effects. First, it changes the spectral energy distribution in the UV because of strong metal line absorption in the outer atmosphere (“line-blanketing”). An example is given in Fig. 3. While the UV flux is reduced, the physical requirement of radiative equilibrium and conservation of the total flux leads to an increase of the emergent flux at optical and IR wavelengths relative to the unblanketed case. This increase comes from the fact that

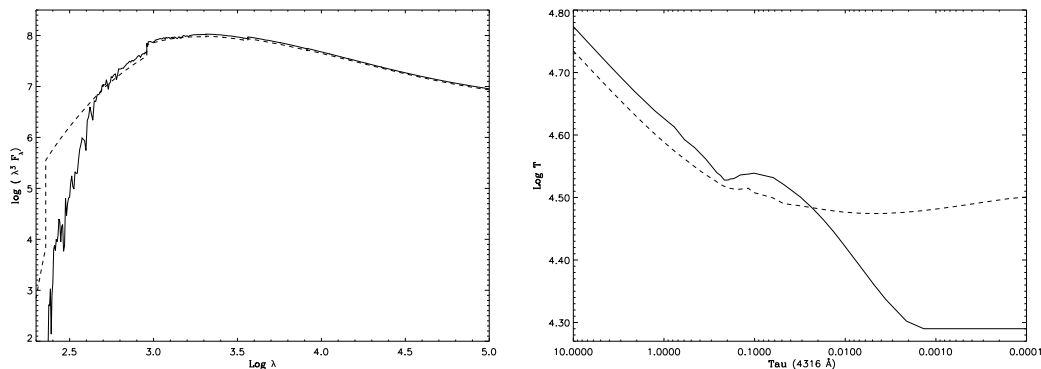


FIGURE 3. Effects of metal line blanketing. Left: Emergent flux of a NLTE hydrodynamic O-star model of $T_{eff}=40,000\text{K}$ with (solid) and without (dashed) metal line blanketing. Right: Local kinetic temperature as a function of monochromatic optical depth at blue wavelength for the same two models. The photospheric backwarming as discussed in the text as the result of blanketing is clearly seen. The NLTE code FASTWIND (Puls et al. (2005)) was used for the calculations.

a significant fraction of the photons absorbed in the outer layers are emitted back to the inner photosphere providing additional energy input and, thus, heating the deeper photospheres. This second “backwarming” effect increases the local kinetic temperature (see Fig. 3), which then leads to stronger photospheric continuum emission and modifies diagnostically important ionization equilibria such as HeI/II, which are used for the determination of T_{eff} . Fig. 4 demonstrates how the HeI/II ionization equilibrium is shifted towards lower T_{eff} because of the backwarming effect. At the same time, the pressure-broadened wings of the Balmer lines (the standard diagnostic for $\log g$) become weaker, because the millions of metal lines increase the radiative acceleration g_{rad} and decrease the effective gravity $g_{eff} = g - g_{rad}$. As a result higher gravities are needed to fit the Balmer lines (see Fig. 4) in addition to the lower temperatures obtained from the helium ionization equilibrium. In summary, the use of blanketed models leads to systematic shifts in the $(\log g, \log T_{eff})$ - plane towards lower temperatures and higher gravities. For stars with known distances to be analyzed this means lower luminosities and lower masses. We also note that the presence of dense stellar wind envelopes increases the effects of backwarming (see Hummer (1982), Abbott & Hummer (1985)). In addition, stellar winds also affect the strengths of diagnostically crucial HeI absorption lines by contaminating the absorption with stellar wind line emission (Gabler, Gabler, Kudritzki et al. (1989), Sellmaier et al. (1993), Repolust et al. (2004)).

The combined effects of line blanketing and backwarming affect also the ionizing fluxes. Amazingly, for the ionization of hydrogen the changes are very small as the effects of blanketing and backwarming balance each other. However, the ionization of ions with absorption edges shorter than the one for hydrogen is significantly affected (see Kudritzki (2002), Martins et al. (2005a)).

Over the last years very powerful and user friendly software packages to calculate NLTE model atmospheres with metal line blanketing have been developed, which are now available to the astronomical community and which have been intensively applied for spectral diagnostics of hot massive stars. At Munich University Observatory the codes “WM-Basic” (Pauldrach, Lennon & Hoffmann (2001)) and “FASTWIND” (Puls et al. (2005)) were developed in partial collaboration with the authors of this article and at Pittsburgh the code “CMFGEN” is the result of intensive work by John Hillier and collabo-

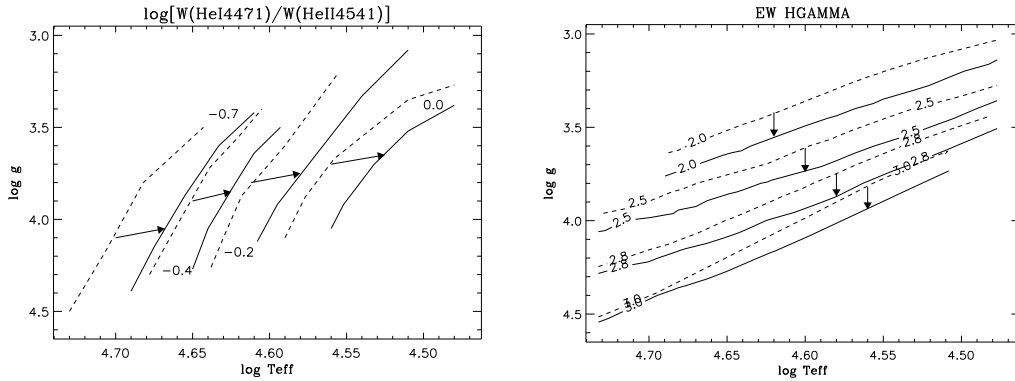


FIGURE 4. Effects of metal line blanketing on the stellar diagnostics. Plotted are the isocontours of $\log [W_{\lambda}(\text{HeI}4471)/W_{\lambda}(\text{HeII}4542)]$ (left) and $W_{\lambda}(\text{H}_{\gamma})$ (right) in the $(\log g, \log T_{\text{eff}})$ - plane. Dashed isocontours are unblanketed models, solid are blanketed. Vectors indicate the shifts caused by the effects of NLTE metal line blanketing. As for the previous figures the calculations were done with the NLTE code FASTWIND (Puls et al. (2005)).

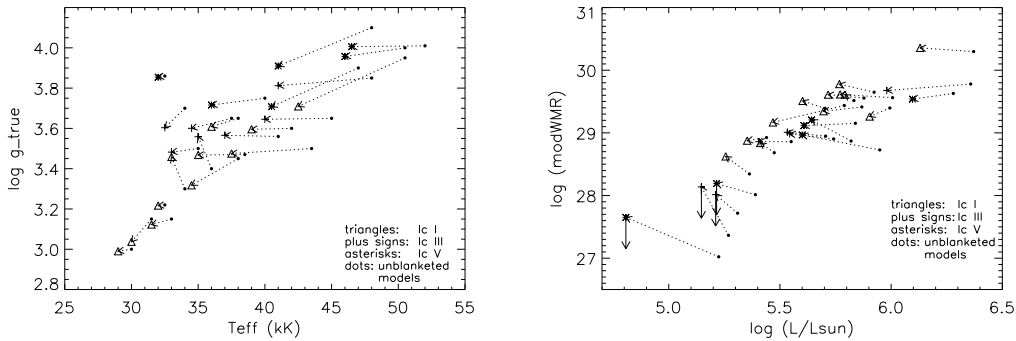


FIGURE 5. Effects of metal line blanketing on the stellar diagnostics. Left: Shifts of the location of individual O-stars in the $(\log g, \log T_{\text{eff}})$ -plane caused by the use of metal line blanketed models in the analysis of the hydrogen and helium optical line spectrum. Right: Shifts of modified stellar wind momenta (see section 7) as a function of luminosity. (From Repolust et al. (2004)).

rators (Hillier et al. (2003)). Ivan Hubeny and Thierry Lanz have developed “TLUSTY” (Lanz & Hubeny (2003)), which does not include the hydrodynamics of winds but can be applied in all cases, where the stellar winds are weak.

3. The effective temperature scale of O-stars

With the new generation of NLTE metal line blanketed model atmospheres available quite a number of very detailed spectroscopic studies of O-stars have been published over the last five years. While the diagnostic methods used are generally still the same as in the earlier work by Kudritzki (1980), Kudritzki et al. (1983), Kudritzki et al. (1989), Kudritzki & Hummer (1990), Herrero, Kudritzki, et al. (1992), which was based on a first generation of hydrostatic NLTE model atmospheres with hydrogen and helium opacity only, the results coming out of the new work are substantially different because of the tremendous improvements of the model atmospheres. Since the effects of metal line blan-

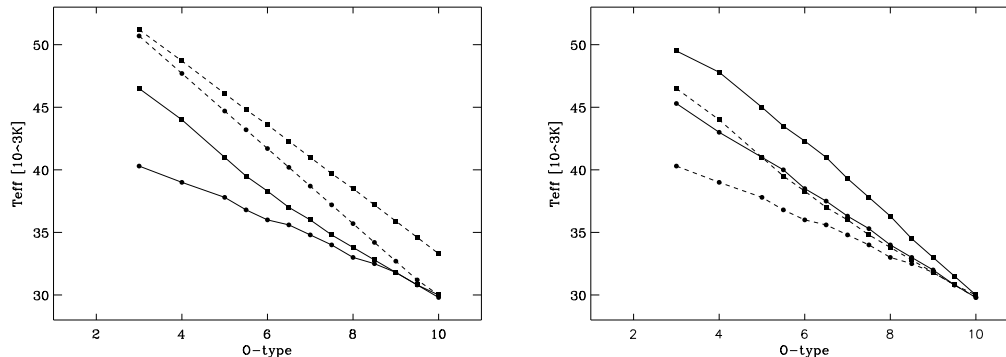


FIGURE 6. Left: Effective temperature as a function of spectral type for Milky Way O-stars. Supergiants are plotted as circles and giants and dwarfs as squares. The new scales are represented by the solid curves, and the old scales by the dashed curves. For discussion see text. Right: The new effective temperature scale of O-stars in the SMC (solid) relative to the Milky Way (dashed). (From Massey, Puls, Pauldrach et al. (2005)).

keting depend on the stellar metallicity, we will discuss O-stars in the solar neighborhood of the Milky Way and in the Magellanic Clouds separately.

3.1. O-stars in the Milky Way

Milky Way O-stars have been studied by Pauldrach, Lennon & Hoffmann (2001), Herrero et al. (2002), Martins et al. (2002), Bianchi & Garcia (2002), Garcia & Bianchi (2004), Repolust et al. (2004), Markova et al. (2004), Martins et al. (2005a), Mokiem et al. (2005), Bouret et al. (2005). The result of all these studies with regard to the effective temperature scale is quite dramatic. An example is given by Fig. 5, which displays the shifts in the ($\log g$, $\log T_{eff}$)-plane of individual O-stars, when the classical analysis of hydrogen and helium lines based on unblanketed model atmospheres is replaced by blanketed models. As to be expected from the previous section, the use of blanketed models leads to cooler effective temperatures, which is simply caused by the fact that blanketed models have higher intrinsic local photospheric temperatures and thus models with lower T_{eff} are required to fit the observed helium ionization equilibrium. In addition, blanketed models have a lower local gas pressure and, thus, a higher gravity is generally needed to fit the pressure broadened Balmer lines.

While systematic effects towards somewhat lower effective temperatures and higher gravities, were always expected in previous work based on unblanketed models, the large shifts as displayed in Fig. 5 come as a surprise. We note that the effects are strongest for very hot objects and low gravity supergiants, which have very strong and dense winds affecting the helium ionization equilibrium additionally by the mechanisms discussed above. In some cases we encounter effective temperature changes of the order of 10 to 15 percent. Based on the work by Repolust et al. (2004), Massey, Puls, Pauldrach et al. (2005) have introduced a new effective temperature scale for Milky Way O-stars, which is displayed in Fig. 6 and compared to the old scale by Vacca et al. (1996). We realize that, in particular for supergiants, the differences between the two scales are dramatic. A very similar new effective temperature scale has also been introduced independently by Martins et al. (2005a) based on a comprehensive study of a large sample of O-stars.

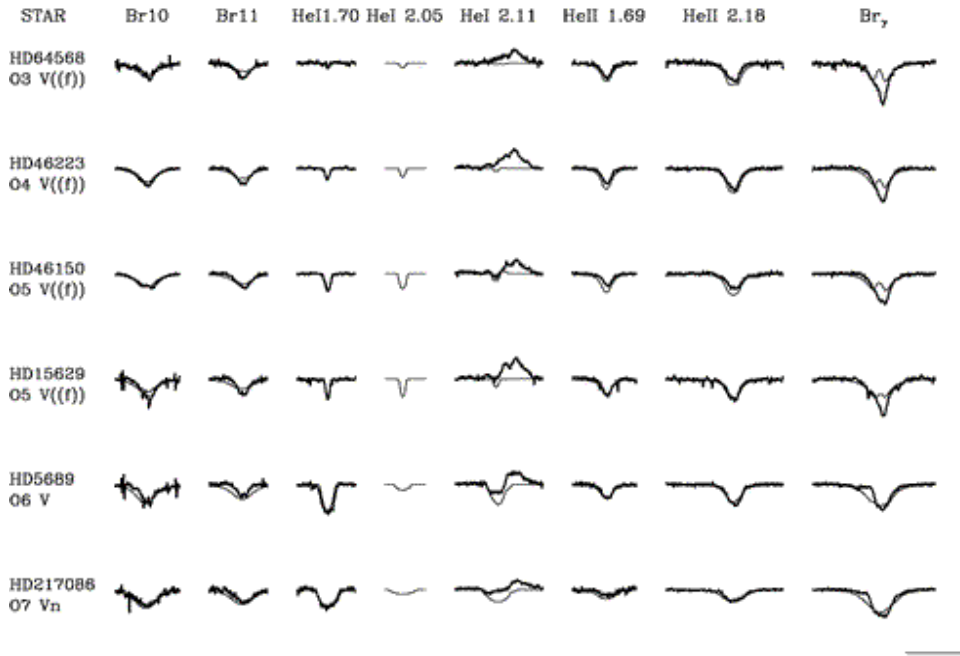


FIGURE 7. Model atmosphere fits of IR hydrogen and helium lines to determine stellar parameters. Note that HeI 2.11 μ is blended by nitrogen lines not included in the calculations. Br $_{\gamma}$ is blended by HII region emission in some cases. (From Repolust et al. (2005)).

3.2. Quantitative IR spectroscopy of O-stars

Massive stars are frequently found in star forming regions heavily obscured by interstellar dust. In such a situation IR spectroscopy is the only way to obtain information. In the galactic center Najarro et al. (1994), Najarro et al. (1997), Figer et al. (1998), Najarro et al. (2004) (see also the contribution by Don Figer in this volume) have demonstrated how quantitative IR spectroscopy can be used to determine the stellar parameters of very extreme supergiants and Wolf-Rayet stars. Similar work has now been carried more recently for “normal” O-stars with the goal to find out whether the analysis of the hydrogen and helium lines in the IR yields accurate information about stellar parameters consistent with the ones obtained from the analysis of the optical spectrum. Hanson, Kudritzki, Kenworthy et al. (2005) and Repolust et al. (2005) have used Subaru H and K band spectra of high S/N to study a large sample of O-stars with very encouraging results showing that IR spectroscopy leads to effective temperatures, gravities and mass-loss rates practically identical with those determined from optical spectra (Fig. 7 gives an example). In parallel, Lenorzer et al. (2004) have carried out a systematic model atmosphere study of the IR spectral diagnostics for normal O-stars focussing on both stellar lines as well as HII region emission lines. It is obvious from this new work that for future investigations of massive stars in dense and highly obscured star forming regions quantitative IR spectroscopy has an enormous potential.

3.3. Effects of metallicity. The effective temperature scale of O-stars in the Magellanic Clouds

From the discussion in section 2 it is clear that metallicity must have an influence on the strengths of blanketing effects and, thus, the effective temperature scale of O-stars. The

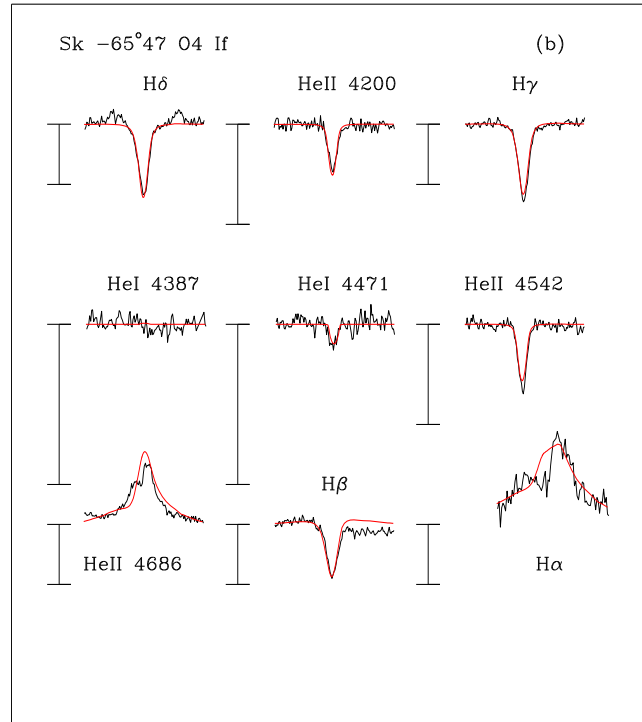


FIGURE 8. Model atmosphere fits of optical hydrogen and helium lines of an O-star in the LMC to determine stellar parameters. (From Massey, Bresolin, Kudritzki et al. (2004)).

ideal laboratory to investigate the metallicity dependence are the Magellanic Clouds because of their lower metallicity relative to the Milky Way. Massey, Bresolin, Kudritzki et al. (2004) and Massey, Puls, Pauldrach et al. (2005) and, independently, Mokiem et al. (2004) and Mokiem et al. (2006a) have carried out a systematic and comprehensive spectroscopic study of O-stars in the clouds. Fig. 6 and Fig. 8 describe the work done by Massey and collaborators. From a detailed fit of the optical hydrogen and helium lines and HST and FUSE UV spectra they were able to determine stellar parameters and stellar wind properties. The result with regard to the effective temperature scale is striking and in agreement with the expectation based on model atmosphere theory. For a given spectral type defined by the relative strengths of HeI and HeII lines O-stars at lower metallicity are significantly hotter than their galactic counterparts, a result which is also clearly confirmed by the work of Mokiem and collaborators. For the determination of IMFs in other galaxies based on spectral classification or for the investigation of the stellar content of galaxies or HII-regions based on nebular emission line analysis this is an important effect to be taken into account. Also for the study of integrated spectra of starburst galaxies the metallicity dependence of the effective temperature scale might be important.

3.4. *Systematic effects depending on the analysis method*

In the work discussed so far effective temperatures and gravities have been determined from the fit of the He I/II ionization equilibrium of optical or IR helium lines and the

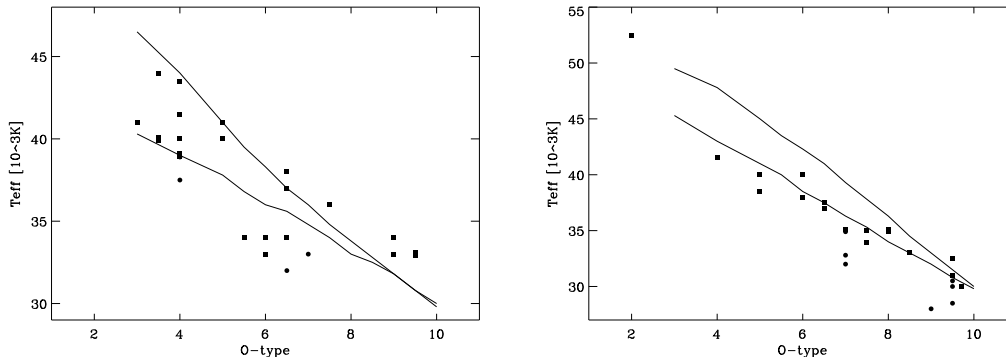


FIGURE 9. O-star effective temperature scales according to Massey, Puls, Pauldrach et al. (2005) for the Milky Way (left) and the SMC (right) based on the analysis of the HeI/II ionization equilibrium at optical wavelengths. Overplotted are the results of spectral analyses using UV metal lines as temperature indicator (see text for the data sources). Supergiants are plotted as circles giants and dwarfs as squares.

Balmer lines. Since O-stars are UV bright and hundreds of photospheric lines can be identified in high resolution UV spectra (IUE, HST, ORFEUS, FUSE), it is tempting to use this spectral range to obtain independent information about the stellar parameters. As it turns out, it is difficult to constrain gravities solely through the UV, however, there are ionization equilibria such as Fe IV/V/VI or CIII/IV which can be used for a determination of temperatures. For Milky Way O-stars such work has been carried out by Pauldrach, Lennon & Hoffmann (2001), Bianchi & Garcia (2002), Garcia & Bianchi (2004), and Bouret et al. (2005). As shown in Fig. 9 significantly lower T_{eff} are obtained in some cases from the UV lines compared to optical/IR HeI/II lines. In particular, the work by Bianchi & Garcia (2002) and Garcia & Bianchi (2004) has resulted in very low effective temperatures.

A similar result has been obtained by Heap, Lanz & Hubeny (2006) for SMC O-stars mostly of luminosity class V. Fig. 9 shows their results compared to the effective temperature scale obtained by Massey, Bresolin, Kudritzki et al. (2004) and Massey, Puls, Pauldrach et al. (2005). Fig. 9 also displays the results found by Crowther et al. (2002), Hillier et al. (2003), Bouret et al. (2003), and Evans et al. (2004), which show a less extreme but similar trend.

This indication of a systematic effect depending on the analysis method deserves a very careful and systematic future investigation. What is needed is a comprehensive simultaneous UV, optical, IR analysis of all the O-stars studied so far. The observational material seems to be available or can be easily obtained. Of course, this will be a time consuming effort requiring a lot of detailed spectroscopic and model atmosphere work. However, it is extremely important that the reasons for these obvious discrepancies are well understood.

4. The effective temperature scale of B and A supergiants

As shown in Fig. 1 massive O-stars evolve into B and later A supergiants. Based on unblanketed, hydrostatic NLTE model atmospheres an effective temperature scale was introduced for galactic B supergiants by McErlean et al. (1998, 1999). More recently, Trundle et al. (2004), Trundle & Lennon (2005), and Crowther, Lennon & Walborn (2005) have analyzed a large sample of Milky Way and SMC B supergiants with the improved

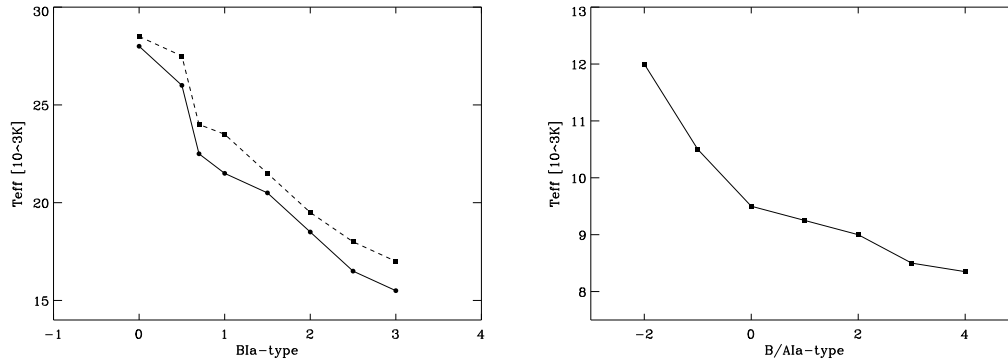


FIGURE 10. The effective temperature scales of early B-supergiants (left, the dashed curve shows the old scale based on unblanketed NLTE models) and late B and early A-supergiants (right) of luminosity class Ia. Note that in the right plot on the abscissa the value of -2 corresponds to spectral type B8.

models and have revised the effective temperature scale for the earliest spectral types of luminosity class Ia. The results are shown in Fig. 10. Note that if the spectral classification scheme introduced by Lennon, D.J. (1997) is used, the effective temperature scale should not depend on metallicity. This is indeed the case, as a comparison of the SMC sample (Trundle & Lennon (2005)) with the MW sample (Crowther, Lennon & Walborn(2005)) shows.

Kudritzki, Bresolin, & Przybilla (2003) have recently introduced an effective temperature scale for late B and early A supergiants of luminosity class Ia and of solar metallicity, which is also displayed in Fig. 10. A discussion of the metallicity dependence can be found in Evans & Howarth (2003).

5. Extragalactic stellar astronomy with B and A supergiants

As shown in Fig. 1 O-stars with masses between 15 to 40 M_{\odot} evolve into supergiants of spectral B and A. Although not as massive and luminous as the most massive O-stars, these stars are the brightest “normal” stars at visual light with absolute magnitudes $-7.0 \geq M_V \geq -9.5$, see Bresolin (2003). (By “normal” we mean stars evolving peacefully without showing signs of eruptions or explosions, which are difficult to handle theoretically and observationally). While O-stars emit most of their radiation in the extreme and far UV because of their high atmospheric temperature, late B and early A supergiants are cooler and their bolometric corrections are much smaller because of Wien’s law so that their brightness at visual light reaches a maximum value during stellar evolution. It is this enormous intrinsic brightness at visual light, which makes them extremely interesting for extragalactic studies far beyond the Local Group.

During their smooth evolution from the left to the right in the HRD massive stars are crossing the temperature range of late B and early A-supergiants in a timescale on the order of several 10^3 years (Meynet & Maeder (2000)). During this short evolutionary phase stellar winds with mass-loss rates of the order $10^{-6} M_{\odot} \text{ yr}^{-1}$ or less (Kudritzki & Puls (2000)) do not have enough time to reduce the mass of the star significantly so that the mass remains constant. In addition, as Fig. 1 shows, the luminosity stays constant as well. The fact that the evolution of these objects can very simply be described by constant mass, luminosity and a straightforward mass-luminosity relation-

ship makes them a very attractive stellar distance indicator, as we will explain later in this review.

As evolved objects the blue supergiants are older than their O-star progenitors, with ages between 0.5 to 1.3×10^7 years (Meynet & Maeder (2000)). All galaxies with ongoing star formation or bursts of this age will show such a population. Because of their age they are spatially less concentrated around their place of birth than O-stars and can frequently be found as isolated field stars. This together with their intrinsic brightness makes them less vulnerable as distance indicators against the effects of crowding even at larger distances, where less luminous objects such as Cepheids and RR Lyrae start to have problems.

With regard to the crowding problem we also note that the short evolutionary time of 10^3 years makes it generally very unlikely that an unresolved blend of two supergiants with very similar spectral types is observed. On the other hand, since we are dealing with spectroscopic distance indicators, any contribution of unresolved additional objects of different spectral type is detected immediately, as soon as it affects the total magnitude significantly.

Thus, it is very obvious that blue supergiants seem to be ideal to investigate the properties of young populations in galaxies. They can be used to study reddening laws and extinction, detailed chemical composition, i.e. not only abundance patterns but also gradients of abundance patterns as a function of galactocentric distance, the properties of stellar winds as function of chemical composition and the evolution of stars in different galactic environment. Most importantly, as we will demonstrate below, they are excellent distance indicators.

6. Quantitative stellar spectroscopy beyond the Local Group

Enormous progress has been made over the last years in the development of accurate NLTE spectral diagnostics of B and A supergiants. Using high resolution and high S/N spectra Urbaneja (2004), Urbaneja et al. (2005b), Trundle et al. (2004), Trundle & Lennon (2005), and Crowther, Lennon & Walborn(2005) have studied early B-supergiants in Local Group galaxies and the Milky Way to determine stellar properties, chemical composition and abundance gradients. For late B and early A supergiants Przybilla et al. (2001a,b,c, 2006) have developed very detailed model atoms for the NLTE radiative transfer diagnostics, which allow for an extremely accurate determination of effective temperature (1%), gravities (0.05 dex), and chemical abundances (0.1 dex). Detailed abundance studies of A supergiants in many Local Group galaxies using these NLTE methods were carried out by Venn et al. (1999, 2000, 2001, 2003) and Kaufer et al. (2004). The analysis technique is similar to O-stars, except that different ionization equilibria are used for the determination of effective temperatures (SiII/III/IV for early B supergiants and OI/II, NI/II, MgI/II, SII/III for late B and early A supergiants, see Kudritzki (2003) for a more detailed description).

6.1. Chemical composition

For extragalactic applications beyond the Local Group spectral resolution becomes an issue. The important points are the following. Unlike the case of late type stars, crowding and blending of lines is not a severe problem for hot massive stars, as long as we restrict our investigation to the visual part of the spectrum. In addition, it is important to realize that massive stars have angular momentum, which leads to usually high rotational velocities. Even for A-supergiants, which have already expanded their radius considerably during their evolution and, thus, have slowed down their rotation, the observed projected

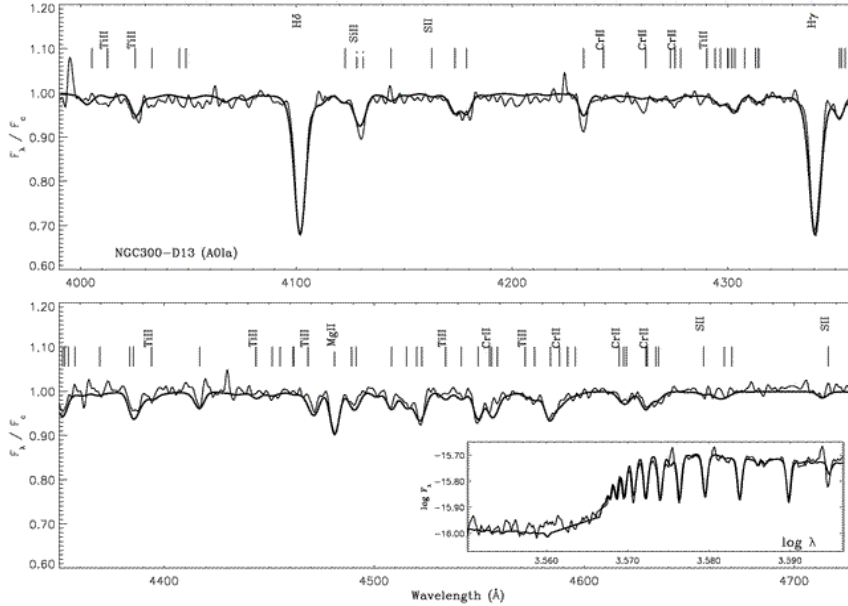


FIGURE 11. Quantitative spectral analysis of an A-supergiant in the Sculptor spiral galaxy NGC 300 at a distance of 2 Mpc. The inset shows the fit of the Balmer jump, which is used to determine T_{eff} . (From Kudritzki, Urbaneja, Bresolin et al. (2006b), see also Bresolin et al. (2002a)).

rotational velocities are still on the order of 30 km s^{-1} or higher. This means that the intrinsic full half-widths of metal lines are on the order of 1 \AA . In consequence, for the detailed studies of supergiants in the Local Group a resolution of 25,000 sampling a line with five data points is ideal. This is indeed the resolution, which has been applied in most of the work referred to above.

However, as we have found out empirically (Przybilla (2002)), degrading the resolution to 5,000 ($\text{FWHM} = 1 \text{ \AA}$) has only a small effect on the accuracy of the diagnostics, as long as the S/N remains high (i.e. 50 or better). Even for a resolution of 2,500 ($\text{FWHM} = 2 \text{ \AA}$) it is still possible to determine T_{eff} to an accuracy of 2 percent, $\log g$ to 0.05 dex and individual element abundances to 0.1.

Bresolin et al. (2001, 2002a, 2002b, 2003, 2006), Urbaneja et al. (2003, 2005a, 2006), Kudritzki, Bresolin, & Przybilla (2003) and Kudritzki, Urbaneja, Bresolin et al. (2006b) have used FORS at the VLT with a resolution of 1,000 ($\text{FWHM} = 5 \text{ \AA}$) to study blue supergiants far beyond the Local Group. The accuracy in the determination of stellar properties at this rather low resolution is still remarkable. The effective temperature (for late B and A supergiants now determined from the Balmer jump rather than from ionization equilibria) is accurate to roughly 4 percent and the determination of gravity based on fitting the broad Balmer lines remains unaffected by the lower resolution and is still good to 0.05 dex. Abundances can be determined with an accuracy of 0.2 dex. In Fig. 11, 12, and 13 we show examples of the detailed spectral fits that can be accomplished. Fig. 13 demonstrates, how important information about the metallicity gradients of the young stellar population in spiral galaxies can be obtained directly from the spectral analysis of blue supergiants.

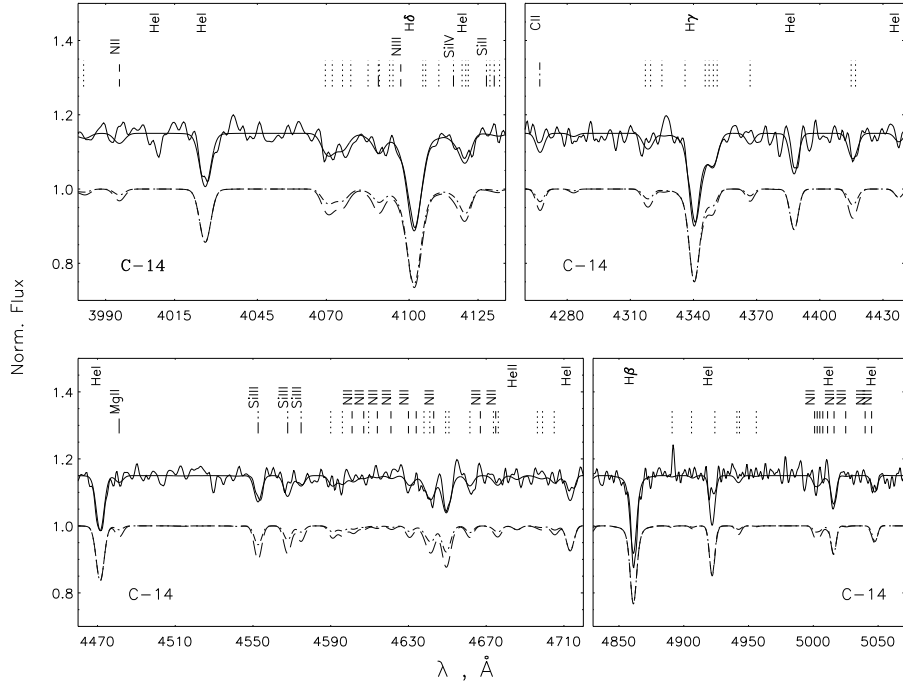


FIGURE 12. Quantitative spectral analysis of an early B-supergiant in the Sculptor spiral galaxy NGC 300. (From Urbaneja et al. (2005a)).

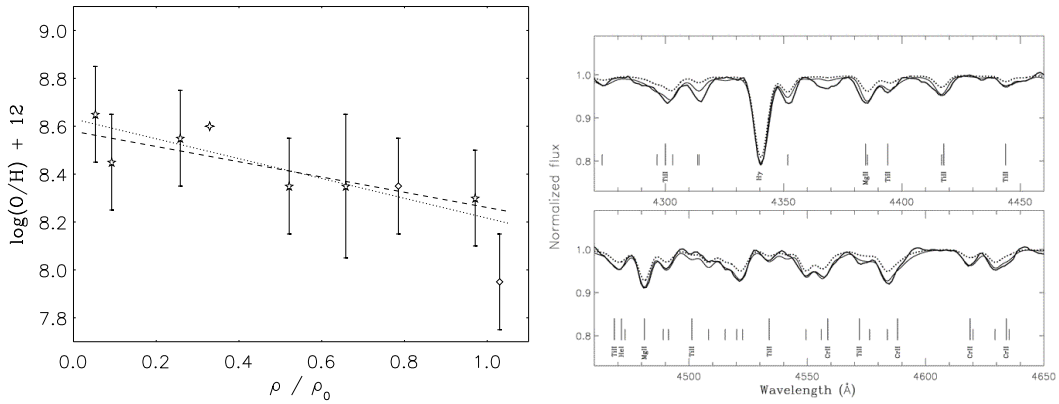


FIGURE 13. Left: the metallicity gradient of the young stellar population in the Sculptor spiral galaxy NGC 300 as determined for quantitative stellar spectroscopy. (From Urbaneja et al. (2005a), Bresolin et al. (2002a,b)). Right: Quantitative spectral analysis of an A-supergiant in the spiral galaxy NGC 3621 at a distance of 7 Mpc. (From Bresolin et al. (2001)).

6.2. Extragalactic distance determinations with the “Flux Weighted Gravity - Luminosity Relationship (FGLR)”

The best established stellar distance indicators, Cepheids and RR Lyrae, suffer from two major problems, extinction and metallicity dependence, both of which are difficult to determine for these objects with sufficient precision. Thus, in order to improve distance determinations in the local universe and to assess the influence of systematic errors there

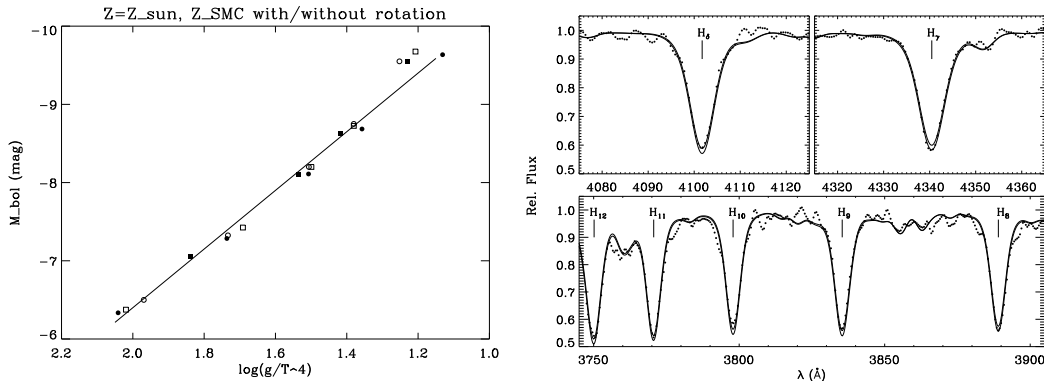


FIGURE 14. Left: The FGLR of stellar evolution models from Meynet et al. (1994) and Meynet & Maeder (2000). Circles correspond to models with rotation, squares represent models without the effects of rotation. Solid symbols refer to galactic metallicity and open symbols represent SMC metallicity. The solid curve corresponds to $a = -3.75$ in the FGLR. Note that gravities are in cgs units and the temperatures are in units of 10^4 K. Right: Fit of the higher Balmer lines of an A-supergiant in the Sculptor galaxy NGC 300 using two atmospheric models with $T_{eff} = 9500$ K and $\log g = 1.60$ (*thick line*) and 1.65 (*thin line*), respectively. The data were taken with FORS at the VLT. For further discussion see Kudritzki, Bresolin, & Przybilla (2003)

is definitely a need for alternative distance indicators, which are at least as accurate but are not affected by uncertainties arising from extinction or metallicity. Blue supergiants are ideal objects for this purpose because of their enormous intrinsic brightness, which makes them available for accurate quantitative spectroscopic studies even far beyond the Local Group using the new generation of 8m-class telescopes and the extremely efficient multi-object spectrographs attached to them (see previous subsection). Quantitative spectroscopy allows us to determine the stellar parameters and thus the intrinsic energy distribution, which can then be used to measure reddening and the extinction law. In addition, metallicity can be derived from the spectra. We emphasize that a reliable *spectroscopic* distance indicator will always be superior, since an enormous amount of additional information comes for free, as soon as one is able to obtain a reasonable spectrum.

A very promising spectroscopic distance determination method based on simple stellar physics is the *Flux-Weighted Gravity – Luminosity Relationship* (FGLR), which was introduced by Kudritzki, Bresolin, & Przybilla (2003). When discussing Fig. 1 in Sect. 1 we noted that massive stars evolve through the domain of blue supergiants with constant luminosity and constant mass. This has a very simple, but very important consequence for the relationship of gravity and effective temperature along each evolutionary track. From

$$L \propto R^2 T_{\text{eff}}^4 = \text{const.}; M = \text{const.} \quad (6.1)$$

follows immediately that

$$M \propto g R^2 \propto L (g/T_{\text{eff}}^4) = \text{const.} \quad (6.2)$$

This means that each object of a certain initial mass on the ZAMS has its specific value of the “flux-weighted gravity” g/T_{eff}^4 during the blue supergiant stage. This value is determined by the relationship between stellar mass and luminosity, which to a good approximation is a power law

$$L \propto M^x . \quad (6.3)$$

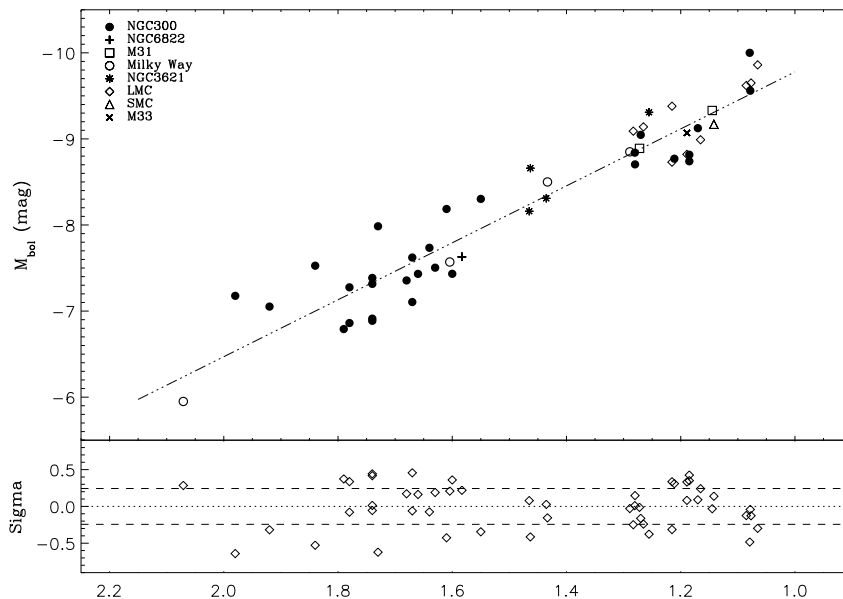


FIGURE 15. The FGLR of B and A supergiants in Local Group galaxies and in the spiral galaxies NGC 300 and NGC 3621 at a distance of 2 and 7 Mpc, respectively. The abscissa is the same as in Fig. 14 (left). (From Kudritzki, Urbaneja, Bresolin et al. (2006b), see also Kudritzki, Bresolin, & Przybilla (2003)). For a discussion, see text.

Inspection of evolutionary calculations with mass-loss, cf. Meynet et al. (1994) and Meynet & Maeder (2000), shows that $x = 3$ is a good value in the range of luminosities considered, although x changes towards higher masses. With the mass – luminosity power law we then obtain

$$L^{1-x} \propto (g/T_{\text{eff}}^4)^x, \quad (6.4)$$

or with the definition of bolometric magnitude $M_{\text{bol}} \propto -2.5 \log L$

$$-M_{\text{bol}} = a \log(g/T_{\text{eff}}^4) + b. \quad (6.5)$$

This is the FGLR of blue supergiants. Note that the proportionality constant a is given by the exponent of the mass – luminosity power law through

$$a = 2.5x/(1-x). \quad (6.6)$$

and $a = -3.75$ for $x = 3$. Mass-loss will depend on metallicity and therefore affect the mass – luminosity relation. In addition, stellar rotation through enhanced turbulent mixing might be important for this relation. In order to investigate these effects we have used the models of Meynet et al. (1994) and Meynet & Maeder (2000) to construct the stellar evolution FGLR, which is displayed in Fig. 14. The result is very encouraging. All different models with or without rotation and with significantly different metallicity form a well defined very narrow FGLR.

In order to verify the existence of the theoretically predicted FGLR Kudritzki, Bresolin, & Przybilla (2003) re-analyzed a large sample of late B and early A supergiants in several Local Group galaxies (high resolution spectra) and in the spiral galaxies NGC 300 (2Mpc) and NGC 3621 (7Mpc) using VLT FORS low resolution spectra as described above. Fig. 14 demonstrates

how precisely the gravities can be determined even at low resolution. The effective temperatures were obtained from the spectral types using the relation displayed in Fig. 10. Taking into account the valid criticism by Evans & Howarth (2003) about the metallicity dependence of the temperature vs. spectral type relationship, Kudritzki, Urbaneja, Bresolin et al. (2006b) used the information about the Balmer jump in the VLT/FORS spectrophotometric data (see Fig. 11) to determine effective temperature and metallicity independently. This new procedure lead to the FGLR shown in Fig. 15. A least square fit yields $a=-3.31$ and $b=13.09$ with a one σ scatter of 0.24 mag. Fixing the slope to the theoretical value $a=-3.75$ we obtain as a zero point $b=-13.73$ with $\sigma=0.25$.

The FGLR as displayed in Fig. 15 is an extremely tight relationship with a scatter comparable to the observed period-luminosity relationships of Cepheids. We conclude that blue supergiants provide a great potential as excellent extragalactic distance indicators. The quantitative analysis of their spectra – even at only moderate resolution – allows the determination of stellar parameters, stellar wind properties and chemical composition with remarkable precision. In addition, since the spectral analysis yields intrinsic energy distributions over the whole spectrum from the UV to the IR, multi-colour photometry can be used to determine reddening, extinction laws and extinction. This is a great advantage over classical distance indicators, for which only limited photometric information is available, when observed outside the Local Group. Spectroscopy also allows to deal with the effects of crowding and multiplicity, as blue supergiants, due to their enormous brightness, are less affected by such problems than for instance Cepheids, which are fainter.

Applying the FGLR method on objects brighter than $M_V = -8$ mag and using multi-object spectrographs at 8 to 10m-class telescopes, which allow for quantitative spectroscopy down to $m_V = 22$ mag, we estimate that with 20 objects per galaxy we will be able to determine distances out to distance moduli of $m - M \sim 30$ mag with an accuracy of 0.1 mag. We emphasize that these distances will not be affected by uncertainties in extinction and metallicity, because we will be able to derive the corresponding quantities from the spectrum.

7. Winds of hot massive stars

All hot massive stars have winds, which are driven by radiation. As emphasized in the introduction these winds are fundamentally important for the spectral diagnostics of massive stars, for their evolution and for the galactic environment. Over the last decades very detailed and refined methods have been developed for the diagnostic of stellar winds and for modelling their hydrodynamics. A comprehensive review describing these methods and summarizing the basic properties of stellar winds was published a few years ago by Kudritzki & Puls (2000) (see also Kudritzki (2000), which was published in these Symposium Series). The mass-loss rates and terminal velocities of these winds are related to the physical parameters of massive hot stars through simple relationships. The stellar wind momentum $\dot{M}v_\infty$ is related to radius R , luminosity L and metallicity Z through

$$\dot{M}v_\infty R^{1/2} \propto L^{1.8} (Z/Z_\odot)^{-0.8} \quad (7.1)$$

This the wind momentum luminosity relationship (WLR), which has been introduced first by Kudritzki, Lennon & Puls (1995). (Note that the left hand side is called the “modified stellar wind momentum”). The physics leading to this relationship has been described in detail in Kudritzki (1998) and Kudritzki (2000). Proportionality constants for

the WLR have been determined by Puls, Kudritzki, Herrero et al. (1996) for O-stars and by Kudritzki et al. (1999) for B and A supergiants. (See also Kudritzki & Puls (2000)).

The terminal velocities v_∞ of the winds of hot massive stars are related to the photospheric escape velocities v_{esc}^{phot} and metallicity through

$$v_\infty \propto v_{esc}^{phot} (Z/Z_\odot)^{-0.15} \quad (7.2)$$

$$v_{esc}^{phot} = (2GM(1 - \Gamma)R^{-1})^{1/2} \quad (7.3)$$

The proportionality constant in Eq. 7.2 is about 2.6 (± 0.5) for O-stars and early B-supergiants but becomes smaller for lower temperatures and is about 1.0 for A-supergiants (see Kudritzki & Puls (2000), but see also the new results discussed below). Γ is the usual distance to the Eddington limit.

7.1. O-star wind momenta based on new diagnostics with metal line blanketed model atmospheres

The proportionality constants for the WLR were based on spectral diagnostics of H_α , which is very sensitive to the strengths of stellar winds and, therefore, regarded as a very good indicator of mass-loss rates (see Kudritzki & Puls (2000)). However, the original work was based on the use of NLTE model atmospheres, which neglected metal line blanketing. It was, therefore, crucially important to repeat the H_α studies of stellar winds with the improved model atmospheres described in the sections before.

Repolust et al. (2004) and Markova et al. (2004) carried out a comprehensive study of O-stars in the Milky Way. Fig. 5 indicates the general trend with regard to the diagnostics of wind momenta. Since the analysis with metal line blanketed NLTE atmospheres yield lower temperatures and, therefore, lower luminosities, the WLR is simply shifted towards lower luminosities. Fig. 16 shows the observed WLR for O-stars. As in Kudritzki & Puls (2000) we include the results of similar diagnostics of Central Stars of Planetary Nebulae (CSPN) (for details see Kudritzki, Urbaneja, & Puls (2006a)) to demonstrate that very obviously the WLR extends to these low mass hot stars in a post-AGB evolutionary stage as well. Repolust et al. (2004) and Markova et al. (2004) discuss the difference between the WLR of dwarfs and supergiants and argue that the theory cannot reproduce this difference. They conclude that the H_α mass-loss rates of supergiants are affected by inhomogeneous stellar wind clumping and in reality are probably close to the ones of dwarfs. To check this hypothesis, we compare with the theoretical wind momenta for O-stars and CSPN calculated by Kudritzki (2002), who used a new theoretical approach for the theory of line driven winds. The result is also shown in Fig. 16. While we find a clear offset between the WLRs of dwarfs and supergiants, the theoretical wind momenta are a little too small in both cases, which would mean that clumping might be important for both dwarfs and supergiants. We will discuss the effects of clumping at the end of this review.

With the new stellar parameters derived with metal line blanketed models there is also a change in the values of photospheric escape velocities. After a first check of all the new results the factor relating terminal velocity with escape velocity appears to be 3.1 rather than 2.6.

7.2. Metallicity dependence

Since the mechanism of driving stellar winds is the absorption of photospheric photon momentum through many thousands of spectral lines, it is clear that the strengths of winds is expected to depend on metallicity. First predictions of the metallicity dependence of both mass-loss rates and terminal velocities were made by Abbott (1982)

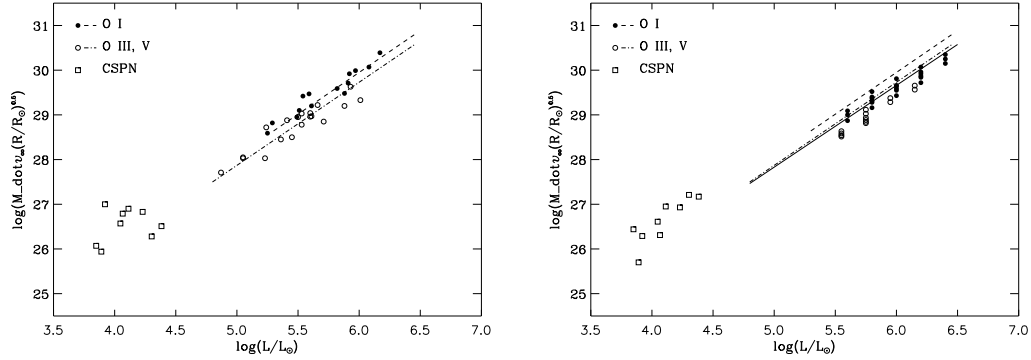


FIGURE 16. Left: Observed wind momenta of O-stars and CSPN as a function of luminosity. Right: Calculated stellar wind momenta for O-stars and CSPN using the theory of line driven winds as developed by Kudritzki (2002). Symbols refer to model calculations. The dashed lines are the regression curves obtained from the observations displayed in the left diagram. The solid line represents the theoretical approach by Vink et al. (2000).

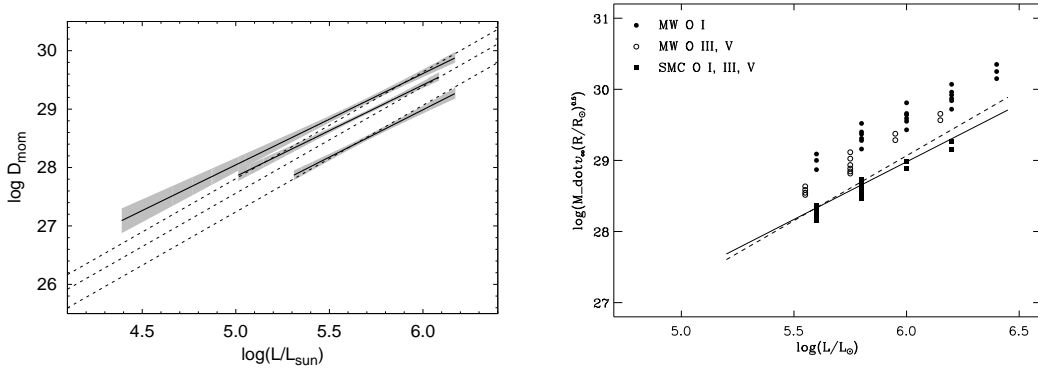


FIGURE 17. Left: Observed wind momenta of O-stars and CSPN as a function of luminosity. The shaded area represent observational results in the MW, LMC, and SMC and the solid lines are the observed WLR regression curves. The dashed curves represent theoretical predictions by Vink et al. (2001) for MW, LMC and SMC metallicities, respectively. (From Mokiem et al. (2006b)). Right: Calculated stellar wind momenta for O-stars and CSPN using the theory of line driven winds as developed by Kudritzki (2002). Symbols refer to model calculations. The solid curve is the observed regression for the SMC from the left diagram. The dashed line represents the theoretical approach for the SMC by Vink et al. (2001).

and Kudritzki et al. (1987), later confirmed and extended by Leitherer et al. (1992). Improved calculations were carried out more recently by Vink et al. (2001) and Kudritzki (2002). Observationally, Puls, Kudritzki, Herrero et al. (1996) analyzed O-stars in the Clouds relative to the Milky way and found a first observational indication for the power law dependence of wind momenta on metallicity. Moreover, Kudritzki & Puls (2000) showed that O-stars in the metal poor SMC have lower lower terminal velocities than their MW counterparts. More recently, Massey, Bresolin, Kudritzki et al. (2004), Massey, Puls, Pauldrach et al. (2005), Evans et al. (2004), Hillier et al. (2003), and Crowther et al. (2002) have clearly confirmed these results. Fig. 17 shows the most recent results obtained by Mokiem et al. (2006b), which indicate excellent agreement with the predictions of the theory.

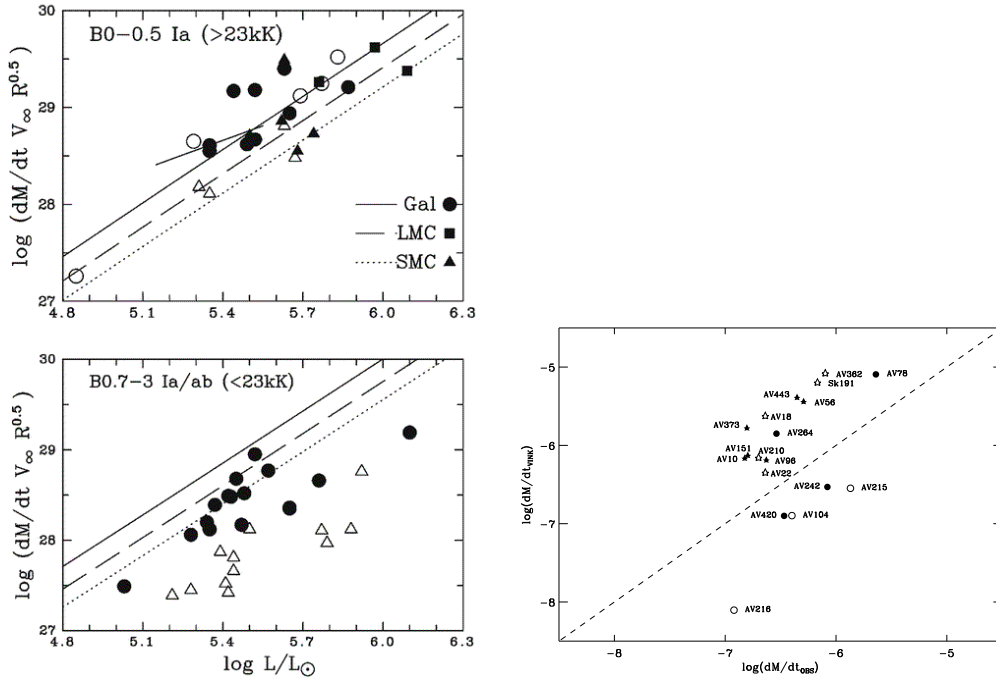


FIGURE 18. Left: Observed wind momenta of B Ia supergiants as a function of luminosity for objects hotter than 23kK (B0-B0.5) (upper panel) and cooler than 23kK (B0.7-3) (lower panel) and for objects in the Galaxy(circles), LMC (squares) and SMC (triangles). Overplotted are wind momenta predicted by the computations by Vink et al. (2000, 2001) for the metallicities of the three galaxies. (from (Crowther, Lennon & Walborn(2005)). Right: Mass-loss rates as predicted by Vink et al. (2001) for SMC B-supergiants compared to observations. Circles represent early type supergiants, stars corresponds to mid types.

7.3. B supergiants

Because of changes in ionization leading to different sets of spectral lines absorbing photospheric photon momentum and driving the stellar winds the WLR is expected to be spectral type dependent. Indeed, Kudritzki et al. (1999) in their study of winds of B and A supergiants found a strong variation of the WLR with spectral type. While early B supergiants seemed to have wind momenta only somewhat weaker than their O-stars counterparts, mid B supergiants showed much weaker winds, whereas A supergiants had stellar wind momenta comparable to the early B spectral types, but a steeper slope of the WLR.

With the new line blanketed models available Trundle et al. (2004), Trundle & Lennon (2005), Urbaneja (2004), Evans et al. (2004) and Crowther, Lennon & Walborn(2005) have re-investigated the wind properties of B-supergiants. In general, the results by Kudritzki et al. (1999) are confirmed. There is still on average a difference in the strengths of wind momenta between early and mid B-spectral types. However, while mass-loss rates for early spectral types are very similar to those obtained with the unblanketed models by Kudritzki et al. (1999), the new values for mid B-supergiants are about a factor of 3 higher on average, but even with this increase they remain significantly lower than those for the earl B types (see Fig. 18). There is a clear metallicity dependence of wind momenta.

As shown in Fig. 18 the theory of line driven winds fails to reproduce these observations. Vink et al. (2000, 2001) predict strong increase of mass-loss rates below 24kK due to

changes of ionization, which is definitely not observed. For the early type supergiants show mass-loss rates much stronger than predicted by the theory. While this can be explained by stellar wind clumping, we believe that that in general more theoretical work for B-supergiant winds is needed.

The ratio between terminal and escape velocities changes as a function of effective temperature showing a similar trend as found by Prinja & Massa (1998), but quantitatively different. For temperatures above 24kK the ratio is 3.4, between 20kK and 24kK it is 2.5 and below 20kK 1.9 is found. In all temperature ranges there is a large scatter around these average values, though.

7.4. *Winds at very low metallicity*

As indicated in the introduction and as discussed in several contributions throughout this symposium there is growing evidence that the evolution of galaxies in the early universe is heavily influenced by the formation of first generations of very massive stars. Thus, it is important to understand the nature of radiation driven winds at very low metallicity. As has been shown by Kudritzki (2002), radiative line forces show a different dependence on optical depth and electron density at very low metallicity, which requires significant modifications of the theoretical description. With those implemented it can be shown that the power law dependence on metallicity of mass-loss rates, wind momenta and velocities breaks down and a much stronger dependence on metallicity is found. For details we refer the reader to the paper by Kudritzki (2002), which also provides ionizing fluxes and predicted UV spectra as a function of metallicity.

7.5. *The effects of rotation and instabilities*

There are many mechanisms, which might lead to an enhancement of mass-loss during stellar evolution. A classical mechanism already taken into account by Pauldrach, Puls, & Kudritzki and Friend & Abbott (1986) is through the centrifugal forces provided by stellar rotation. Kudritzki & Puls (2000), Petrenz & Puls(2000), and Owocki (2005) give an overview about the possible effects. In particular at low metallicities, when massive O-stars are hotter and have much smaller radii and the effects of radiation driven winds become smaller, stellar rotation might become a crucial mechanism not only for stellar mass-loss, but also for stellar evolution (see Marigo et al. (2003), Maeder et al. (2005), Meynet et al. (2005), Hirschi et al. (2005), Ciappini et al. (2006), Meynet et al. (2006)).

Continuum driven winds and their instabilities as very likely encountered in LBV outbursts are another important physically mechanism at least for objects very close to the Eddington limit (see Shaviv (2001), Shaviv (2005), Owocki et al. (2004), Owocki (2005), Smith & Owocki (2006) and the contribution by Nathan Smith at these proceedings).

Stellar pulsations have also been discussed frequently to enhance stellar mass-loss, but as shown by Baraffe et al. (2001) they become less important at low metallicities.

7.6. *The problem of the “weak wind stars”*

UV and optical studies of O-stars in the SMC with luminosities $L \leq 10^{5.5} L_{\odot}$ by Bouret et al. (2003) and Martins et al. (2004) indicated much smaller stellar wind momenta than expected from the theory of radiation driven winds and from a simple extrapolation of the WLR from higher luminosities. More recently, Martins et al. (2005b) have investigated similar “weak wind stars” in the Milky Way and it was found that O-dwarfs with $L \leq 10^{5.2} L_{\odot}$ indeed seem to have much weaker winds than predicted by the theory with a discrepancy of the order of a factor of hundred. It is always simple to speculate about too strong stellar winds. One can invent additional wind driving mechanisms or blame the neglect of clumping in the diagnostics as the reason. However, it is very difficult to explain winds

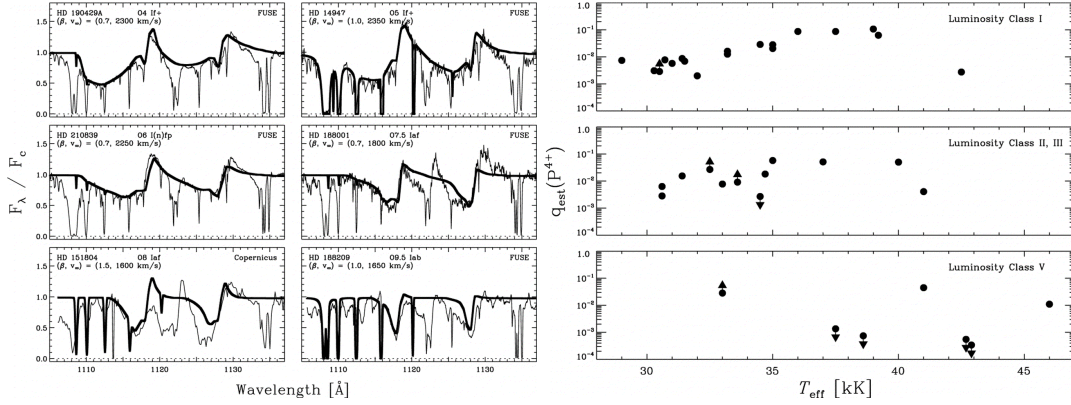


FIGURE 19. Left: Radiative transfer fits of the far UV PV lines of MW O-stars. Right: Ionization fraction of PV as determined from fits of H_α and PV as function of effective temperature. (From Fullerton et al. (2006)).

that are too weak, because the radiative force at a given luminosity is always there and cannot be simply switched off. Thus, it is natural to be suspicious about the accuracy of the spectroscopic diagnostics of these objects.

The determination of mass-loss rates comes mostly from the analysis of UV metal lines, since H_α provides only upper limits in most of the cases. While the diagnostics of those lines have been done in the most careful way with the state-of-the-art model atmospheres described before, the mass-loss rates determined depend crucially on ionization calculations which could severely be affected by the soft X-ray emission of shocks in the stellar wind flow. The authors are aware of this problem and have included effects of shock emission, but it is open at this point whether this treatment of shocks is sufficient. Other possible options - from our point of view less likely - to explain the weak wind stars are discussed by Martins et al. (2005b) and Mokiem et al. (2006b).

7.7. Stellar wind clumping

While H_α is, in principle, a perfect tool to measure mass-loss rates (see Kudritzki & Puls (2000), for discussion and references), the results might be affected by stellar wind clumping. It has been known since long that line driven winds are intrinsically unstable (Owocki et al. 1988, 2004). This might lead to inhomogeneous, clumped winds such as described by Owocki & Runacres (2002) with regions of enhanced density ρ_{cl} and regions, where the density is much lower. In a very simple description, introducing clumping factors f_{cl} similar as in PN diagnostics, the relationship between the average density of the stellar wind flow ρ_{av} and the density in the clumps is then given by $\rho_{cl} = \rho_{av} f_{cl}$. The same relationship holds for the occupation numbers n_i of ions.

Line opacities κ depend on density through $\kappa \propto n_i \propto \rho^x$ and for very small, optically thin clumps the average optical line depth in the wind is given by $\tau_{av} \propto n_i^{av} \propto n_i^{cl} f^{-1} \propto \rho_{av}^x f^{x-1}$. For a dominating ionization stage we have $x = 1$ and the clumping along the line of sight cancels and does not affect the diagnostics. However, bound hydrogen is a minor ionization stage in hot stars depending on recombination from ionized hydrogen with $n_i(H) \propto n_E n_P \propto \rho^2$. Thus, if f_{cl} is significantly larger than one, the H_α mass-loss rate diagnostic is systematically affected and we have $\dot{M}(H_\alpha) = \dot{M}(true) f_{cl}^{1/2}$, following from the fact that $\dot{M}(true) \propto \rho_{av}$.

The spectral diagnostics of clumping is difficult. In principle, it requires the comparison of lines with different exponents x in the density dependence of their opacities. In

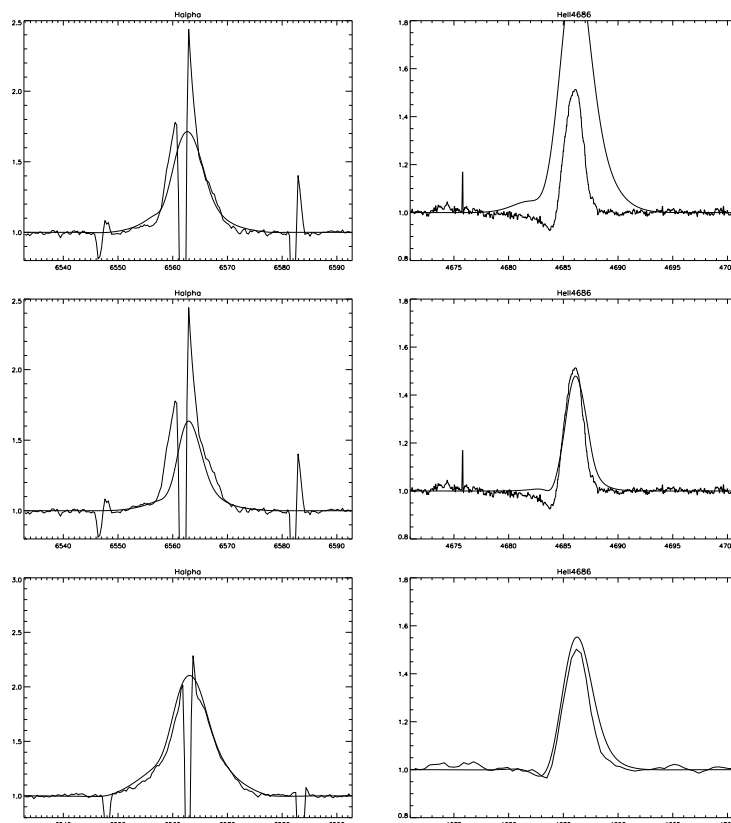


FIGURE 20. Diagnostic of clumping factors in the winds of CSPN. The first two rows show model fits of the H_α (left) and HeII 4686 (right) profile of IC418 with $f_{cl} = 1$ (top row) and $f_{cl} = 50$ indicating enormous clumping. The bottom row shows the same for He2-108 and $f_{cl} = 1$ demonstrating that for this object the wind is very likely homogeneous. Note that the H_α and NII nebular emission lines have been (imperfectly) subtracted. (From Kudritzki, Urbaneja, & Puls (2006a)).

WR-type stars with very dense winds and very strong wind emission lines incoherent electron scattering produces wide emission wings, the strength of which goes with $x \sim 1$. Clumping factors of the order of ten to twenty were found (Hillier (1991), see also contribution by Paul Crowther in these proceedings). This technique does not work for O-type stars, as their winds have much lower density. Also the UV P-Cygni lines of dominating ions provide usually little help, as these lines are mostly saturated and the ionization equilibria are uncertain. However, in most recent work on massive O-stars using FUSE and Copernicus spectra the PV resonance line at 1118 and 1128 Å has been used as an indicator of clumping. The advantage of PV is the low cosmic abundance so that the line is completely unsaturated even when in a dominating ionization stage. Substantial clumping was found (Hillier et al. (2003), Bouret et al., 2003, 2005) with clumping factors of the order of ten.

Very recently, Fullerton et al. (2006) have carried out a comprehensive study of Milky Way O-stars with well observed FUSE PV line profiles producing detailed PV radiative transfer line fits to determine the product $q(P^{4+})\dot{M}$, where $q(P^{4+})$ is the ionization fraction of PV in the ground-state (see Fig.19). Comparing with mass-loss rates derived from H_α (or radio free-free emission) they produced the plot of $q(P^{4+})$ as function of

T_{eff} also shown in Fig.19. Assuming that PV is a dominating ionization stage at all temperatures (and, therefore, $q(P^{4+}) = 1$), they conclude that the H_{α} mass-loss rates are too high by a very large factor up to many orders of magnitudes and implying enormous filling factors.

This is very important work based on the best available diagnostic techniques and poses a very serious problem. The crucial assumption is, of course, $q(P^{4+}) = 1$. Test calculations done by us with the model atmosphere code FASTWIND show that models (without shock emission) predict $q(P^{4+}) = 1$ only for $T_{eff} \leq 35kK$, which would imply a much lower effect than at hotter temperatures. Clearly, for future work a very detailed investigation of the PV ionization (including shock emission) is needed to address this fundamental problem of clumping in O-star winds. The results found by Fullerton et al. (2006) are certainly alarming.

There is an alternative method for the diagnostics of clumping at least for cool O-stars with $T_{eff} \leq 37,000K$, where HeII is a dominant ionization stage. That means for objects with strong winds and HeII 4686 in emission and formed in the wind this line should have a density dependence close to $x = 1$. Its relative strength to H_{α} should allow to constrain f_{cl} .

Kudritzki, Urbaneja, & Puls (2006a) have applied this technique to study clumping in the winds of CSPN with very interesting results (see Fig. 20) yielding clumping factors varying in a range from 50 to 1.

REFERENCES

- ABBOT, D.C. 1982 *ApJ* **259**, 282
 ABBOT, D.C. & HUMMER, D.G. 1985 *ApJ* **294**, 286
 BARAFFE, I., HEGER, A., WOOSLEY, S.E. 2001 *ApJ* **550**, 890
 BARTON, E., DAVE, R., SMITH, J. ET AL. 2004 *ApJ* **604**, L1
 BIANCHI, L. & GARCIA, M. 2002 *ApJ* **581**, 610
 BOURET, J.C., LANZ, T., HILLIER, J.D. ET AL. 2003 *ApJ* **595**, 1182
 BOURET, J.C., LANZ, T., HILLIER, J.D. 2005 *A&A* **438**, 301
 BRESOLIN, F. 2003 *Lect. Notes Phys.* **635**, 149
 BRESOLIN, F., KUDRITZKI, R.P., MENDEZ, R.H., PRZYBILLA, N. 2001 *ApJ* **548**, L149
 BRESOLIN, F., GIEREN, W., KUDRITZKI, R.P., PIETRZYNSKI, G., PRZYBILLA, N. 2002a *ApJ* **567**, 227
 BRESOLIN, F., KUDRITZKI, R.P., NAJARRO, F., GIEREN, W., PIETRZYNSKI, G. 2002b *ApJ* **577**, L107
 BRESOLIN, PIETRZYNSKI, G., GIEREN, W., KUDRITZKI, R.P., PRZYBILLA, N., FOUQUE, P. 2004 *ApJ* **600**, 182
 BRESOLIN, PIETRZYNSKI, G., URBANEJA, M.A., GIEREN, W., KUDRITZKI, R.P., VENN, K.A. 2006 *ApJ* **600**, 182
 BROMM, V., KUDRITZKI, R.P., LOEB, A. 2001 *ApJ*, in press
 CIAPPINI, C., HIRSCHI, R., MEYNET, G. ET AL. 2006 *A&A* **449**, L27
 CROWTHER, P.A., HILLIER, D.J., EVANS, C.J., FULLERTON, A.W., DE MARCO, O., WILLIS, A.J. 2004 *ApJ* **579**, 774
 CROWTHER, P.A., LENNON, D.J., WALBORN, N.R. 2005 *A&A* **446**, 279
 EVANS, C.J., HOWARTH, I. 2003 *MNRAS* **345**, 1223
 EVANS, C.J., CROWTHER, P.A., FULLERTON, A.W., & HILLIER, D.J. 2004 *ApJ* **610**, 1021
 FIGER, D.F., NAJARRO, F., MORRIS, M. ET AL. 1998 *ApJ* **506**, 384
 FRIEND, D. & ABBOTT, D.C. 1986 *ApJ* **202**, 153
 FULLERTON, A., MASSA, D., PRINJA, R. 2006 *ApJ*, in press
 GABLER, R., GABLER, A., KUDRITZKI, R.P., PULS, J., PAULDRACH, A.W.A. 1989 *A&A* **226**, 162
 GABLER, R., KUDRITZKI, R.P., MENDEZ, R.H. 1991 *A&A* **245**, 587

- GABLER, R., GABLER, A., KUDRITZKI, R.P., MENDEZ, R.H. 1992 *A&A* **265**, 656
- GARCIA, M. & BIANCHI, L. 2004 *ApJ* **606**, 497
- HANSON, M.M., KUDRITZKI, R.P., KENWORTHY, M.A., PULS, J., TOKUNAGA, A.T. 2005 *ApJS* **161**, 154
- HEAP, S.R., LANZ, T., HUBENY, I. 2006 *ApJ* **638**, 409
- HERRERO, A., KUDRITZKI, R.P., VILCHEZ, J.M. ET AL. 1992 *A&A* **261**, 209
- HERRERO, A., PULS, J., NAJARRO, F. 2002 *A&A* **396**, 949
- HILLIER, J.D. 1991 *A&A* **247**, 455
- HILLIER, J.D., LANZ, T., HEAP, S.R. ET AL. 2003 *ApJ* **588**, 1039
- HIRSCHI, R., MEYNET, G., MAEDER, A. 2005 *A&A* **443**, 581
- HUMMER, D.G. 1982 *ApJ* **257**, 724
- KAUFER, A., VENN, K.A., TOLSTOY, E., PINTE, C., KUDRITZKI, R.P. 2004 *AJ* **127**, 2723
- KUDRITZKI, R.P. 1980 *A&A* **85**, 174
- KUDRITZKI, R.P. 1998 Proc. "Stellar Astrophysics for the Local Group", eds. A. Aparicio, A. Herrero & F. Sanchez *VIII Canary Islands Winter School in Astrophysics, Cambridge University Press*, 149–261
- KUDRITZKI, R.P. 2000 *STScI Symposium Series Vol. 12*, 202
- KUDRITZKI, R.P. 2002 *ApJ* **577**, 389
- KUDRITZKI, R.P., SIMON, K.P., & HAMANN, W.R. 1983 *A&A* **118**, 245
- KUDRITZKI, R.P., PAULDRACH, A.W.A., PULS, J. 1987 *A&A* **173**, 293
- KUDRITZKI, R.P., CABANNE, K.P., HUSFELD, D. ET AL. 1989 *A&A* **226**, 235
- KUDRITZKI, R.P., HUMMER, D.G. 1990 *AARA* **28**, 303
- KUDRITZKI, R.P., LENNON, D.J., PULS, J. 1995 *Science with the VLT*, eds. J.R. Walsh, J. Danziger, 246
- KUDRITZKI, R.P., PULS, J., LENNON, D.J. ET AL. 1999 *A&A* **350**, 970
- KUDRITZKI, R.P., PULS, J. 2000 *AARA* **38**, 613–666
- KUDRITZKI, R.P. AND THE GSMT SCIENCE WORKING GROUP 2003a *GSMT Science Working Group Report*, <http://www.aura-nio.noao.edu/>
- KUDRITZKI, R.P. 2003 *Lect. Notes Phys.* **635**, 123
- KUDRITZKI, R.P., BRESOLIN, F., PRZYBILLA, N. 2003b *ApJ* **582**, L83
- KUDRITZKI, R.P., URBANEJA, M.A., & PULS, J. 2006a *Proc. IAU Symposium No. 234*, eds. M.J. Barlow & R.H. Mendez, invited paper, in press
- KUDRITZKI, R.P., URBANEJA, M.A., BRESOLIN, ET AL. 2006b *ApJ*, in prep.
- LANZ, T., HUBENY, I. 2003 *ApJ* **465**, 359
- LEITHERER, C., ROBERT, C. & DRISSEN, L. 1992 *ApJ* **401**, 596
- LENNON 1997 *A&A* **317**, 871
- LENORZER, A., MOKIEM, M.R., DEKOTER, A., PULS, J. 2004 *A&A* **422**, 275
- MAEDER, A., MEYNET, G., & HIRSCHI, R. 2005 *ASP Conf. Series* **332**, 3
- MARIGO, P., CHIOSI, C., KUDRITZKI, R.P. 2003 *A&A* **399**, 617
- MARKOVA, N., PULS, J., REPOLUST, T., MARKOV, H. 2004 *A&A* **413**, 693
- MARTINS, F., SCHAERER, D., HILLIER, D.J. 2002 *A&A* **382**, 999
- MARTINS, F., SCHAERER, D., HILLIER, D.J., & HEYDARI-MALAYERI, M. 2004 *A&A* **420**, 1087
- MARTINS, F., SCHAERER, D., HILLIER, D.J. 2005a *A&A* **436**, 1049
- MARTINS, F., SCHAERER, D., HILLIER, D.J. ET AL. 2005b *A&A* **441**, 735
- MASSEY, P., BRESOLIN, F., KUDRITZKI, R.P., PULS, J. & PAULDRACH, A.W.A. 2004 *ApJ* **608**, 1001
- MASSEY, P., PULS, J., PAULDRACH, A.W.A., BRESOLIN, F., KUDRITZKI, R.P., & SIMON, T. 2005 *ApJ* **627**, 477
- MCERLEAN, N.D., LENNON, D.J., DUFTON, P.L. 1998 *A&A* **329**, 613
- MCERLEAN, N.D., LENNON, D.J., DUFTON, P.L. 1999 *A&A* **349**, 553
- MEYNET, G., MAEDER, A., SCHALLER, G., SCHAERER, D., CHARBONNEL, C. 1994 *A&AS* **103**, 97
- MEYNET, G. & MAEDER, A. 2000 *A&A* **361**, 101
- MEYNET, G., MAEDER, A., & EKSTRÖM, S. 2005 *ASP Conf. Series* **332**, 228
- MEYNET, G., EKSTRÖM, S., & MAEDER, A. 2006 *A&A* **447**, 623

- MOKIEM, M.R., MARTIN-HERNANDEZ, N.L., LENORZER, A., DEKOTER, A., TIELENS, A.G.G.M. 2004 *A&A* **419**, 319
- MOKIEM, M.R., DEKOTER, A., PULS, J. ET AL. 2005 *A&A* **441**, 711
- MOKIEM, M.R., DEKOTER, A., EVANS, C. ET AL. 2006a *A&A*, in press
- MOKIEM, M.R., DEKOTER, A., EVANS, C. ET AL. 2006b *A&A*, in press
- NAJARRO, F., HILLIER, D.J., KUDRITZKI, R.P. ET AL. 1994 *A&A* **285**, 573
- NAJARRO, F., KUDRITZKI, CASSINELLI, J.P., STAHL, O., HILLIER, D.J. 1996 *A&A* **306**, 892
- NAJARRO, F., KRABBE, A., GENZEL, R., LUTZ, D., KUDRITZKI, R.P., & HILLER, D.J. 1997 *A&A* **325**, 700
- NAJARRO, F., FIGER, D.F., HILLIER, D.J., KUDRITZKI, R.P. 2004 *ApJ* **611**, L105
- OWOCKI, S.P., CASTOR, J.I., RYBICKI, G.B. 1988 *ApJ* **335**, 914
- OWOCKI, S.P., RUNACRES, M.C. 2002 *A&A* **381**, 1015
- OWOCKI, S., GAYLEY, K., SHAVIV, N. 2004 *ApJ* **616**, 520
- OWOCKI, S. 2005 *ASP Conf. Series* **332**, 169
- PAULDRACH, A.W.A., PULS, J., KUDRITZKI, R.P. 1986 *A&A* **164**, 86
- PAULDRACH, A.W.A., LENNON, M., HOFFMANN, T. 2001 *A&A* **375**, 161
- PETRENZ, P. & PULS, J. 2000 *A&A* **358**, 956
- PRINJA, R.K., & MASSA, D. 1998 *ASP Conf. Series* **131**, 218
- PRZYBILLA, N. 2002 *PhD Thesis, Ludwig-Maximilians-Universität München*
- PRZYBILLA, N., BUTLER, K., BECKER, S.R., KUDRITZKI, R.P. 2001a *A&A* **369**, 1009
- PRZYBILLA, N., BUTLER, K., KUDRITZKI, R.P. 2001b *A&A* **379**, 936
- PRZYBILLA, & N., BUTLER, K. 2001c *A&A* **379**, 995
- PRZYBILLA, N., BUTLER, K., BECKER, S.R., KUDRITZKI, R.P. 2006 *A&A* **445**, 1099
- PULS, J., KUDRITZKI, R.P., HERRERO, A. ET AL. 1996 *A&A* **305**, 171
- PULS, J., URBANEJA, M.A., VENERO, R. ET AL. 2005 *A&A* **435**, 669
- REPOLUST, T., PULS, J., HERRERO, A. 2004 *A&A* **415**, 349
- REPOLUST, T., PULS, J., HANSON, M.M., KUDRITZKI, R.P., & MOKIEM, M.R. 2005 *A&A* **440**, 261
- RIX, S., PETTINI, M., LEITHERER, C., BRESOLIN, F., KUDRITZKI, R.P., STEIDEL, C. 2004 *ApJ* **615**, 98
- SCHAERER, D. 2003 *A&A* **397**, 527
- SELLMAIER, F., PULS, J., KUDRITZKI, R.P., GABLER, A., & GABLER, R. 1993 *A&A* **273**, 533
- SHAVIV, N.. 2001 *ApJ* **594**, 1093
- SHAVIV, N.. 2005 *ASP Conf. Series* **332**, 180
- SMITH, N. & OWOCKI, S. 2006 *ApJ*, submitted
- TRUNDLE, C., LENNON, D.J., PULS, J., & DUFTON, P.L. 2004 *A&A* **417**, 217
- TRUNDLE, C., LENNON, D.J. 2005 *A&A* **434**, 677
- URBANEJA, M.A. 2004 *Thesis, University of La Laguna, Instituto Astrofisica de Canarias, Spain*
- URBANEJA, M.A., HERRERO, A., BRESOLIN, F., KUDRITZKI, R.P., GIEREN, W., PULS, J. 2003 *ApJ* **584**, L73
- URBANEJA, M.A., HERRERO, A., BRESOLIN, F., KUDRITZKI, R.P., GIEREN, W., PULS, J., PRZYBILLA, N., NAJARRO, F., PIETRZYNSKI, G. 2005a *ApJ* **622**, 862
- URBANEJA, M.A., HERRERO, A., KUDRITZKI, R.P., NAJARRO, F., SMARTT, S.J., PULS, J., LENNON, D.J., CORRAL, L.J. 2005b *ApJ* **635**, 311
- URBANEJA, M.A., KUDRITZKI, R.P., BRESOLIN, ET AL. 2006 *ApJ*, in prep.
- VACCA, W.D., GARMANY, C.D., SHULL, J.M. 1996 *ApJ* **460**, 914
- VENN, K.A. 1999 *ApJ* **518**, 405
- VENN, K.A., MCCARTHY, J.K., LENNON, D., PRZYBILLA, N., KUDRITZKI, R.P., LEMKE, M. 2000 *ApJ* **541**, 610
- VENN, K.A., LENNON, D., KAUFER, A., MCCARTHY, J.K., PRZYBILLA, N., KUDRITZKI, R.P., LEMKE, M. 2001 *ApJ* **547**, 765
- VENN, K.A., TOLSTOY, E., KAUFER, A., SKILLMAN, E.D., CLARKSON, S.M., SMARTT, S.J., LENNON, D.J., KUDRITZKI, R.P. 2003 *ApJ* **547**, 765
- VINK, J.S., DE KOTER, A., LAMERS, H.J.G.L.M. 2000 *A&A* **362**, 295
- VINK, J.S., DE KOTER, A., LAMERS, H.J.G.L.M. 2001 *A&A* **369**, 574